INTERCOMPARISON OF MEDIUM-ENERGY NEUTRON ATTENUATION IN IRON AND CONCRETE (5)

Hideo Hirayama
KEK, High Energy Accelerator Research Organization
1-1 Oho, Tsukuba, Ibaraki, 305-0801 Japan

Attenuation Length Sub-working Group
Japan

Abstract

Based on results presented at SATIF-6, problems were revised and sent by the Japanese Working Group to the participants of this action for re-calculation. To determine their energy dependence, 50 and 100 GeV neutrons were then added as the source neutrons. The secondary neutron spectrum for 90°, which was produced by 24 GeV protons on an Hg target, was added as the secondary neutron source. The purpose was to determine the dependence of the attenuation length of secondary neutrons on their spectra.

This paper presents a comparison of the neutron attenuation length of iron and concrete. Results reviewed include those recently (April 2004) sent by three groups to the organiser and those presented at previous SATIF meetings. The paper also discusses themes evoked from this comparison, which should be investigated in the future.

Introduction

Neutron attenuation at a high energy (above a few GeVs) is not supposed to depend on the energy. Its energy dependence below this energy, especially below 1 GeV, is not well understood. The desire is to reach a consensus on the behaviours of neutrons inside various materials. Such a consensus is necessary in order to agree on definitions of the attenuation length, which is very important for shielding calculations involving high-energy accelerators. One such attempt was made by Japanese attendants of SATIF-2, who proposed to compare various computer codes and data on the attenuation of medium-energy neutrons inside iron and concrete shields (cited as a suitable action for SATIF). From the results for neutrons below 400 MeV presented at SATIF-3 [1], it has become clear that neutrons above 20 MeV are important for understanding that the attenuation length and the geometry (planar or spherical) does not substantially affect the results. The attenuation length of neutrons above 20 MeV was compared with the planer geometry for secondary neutrons produced by medium-energy protons at SATIF-4 [2]. Although attenuation lengths varied, all of the results showed the same tendency for an attenuation length increase and neutron energy increase up to 10 GeV [2,3,4]. From the results presented at SATIF-4, SATIF-5 and SATIF-6, it is clear that the attenuation length of secondary neutrons depends strongly on their spectra.

Considering previous SATIF results, problems were revised for re-calculation by the Japanese Working Group and sent to the participants of this action. To determine their energy dependence, 50 and 100 GeV neutrons were then added as source neutrons. The secondary neutrons emitted at 90° from an Hg target [4] bombarded by 24 GeV protons, which were calculated by F. Maekawa [5] using NMTC/JAM [6], were also added as source neutrons.

Results from the three groups were sent to the organiser by the end of April 2004. This paper presents a comparison of the neutron attenuation lengths of iron and concrete, including the results presented at previous meetings and the future themes resulting from this comparison.

Problems involving the intercomparison (5)

Considering the results presented at SATIF-6 [4], the following revised problems were proposed for calculation using various codes and their databases. Secondary neutrons produced from an Hg target by 24 GeV protons at 90° were also added, which were calculated by F. Maekawa using NMTC/JAM [6].

Attenuation calculation

Source neutron energy

a) Source neutrons are uniformly distributed within the following energy regions: 40-50 MeV, 90-100 MeV, 180-200 MeV, 375-400 MeV, 1 GeV, 1.5 GeV, 3 GeV, 5 GeV, 10 GeV, 50 GeV and 100 GeV.

b) Secondary neutrons at 90° from an Fe target (5 cm diameter, 5 cm length) and the following: from 200 MeV protons, from 500 MeV protons, from 1 GeV protons, from 3 GeV protons and from 5 GeV protons (Figure 1).

c) Secondary neutrons in various directions from an Hg target with a Pb moderator (120 cm diameter, 120 cm length) are shown in Figure 2 with 3 GeV protons.

d) Secondary neutrons at 90° from an Hg target shown with 24 GeV protons in Figure 2.

Figure 1. Secondary neutrons at 90° from an iron target bombarded by protons (FLUKA calculations)

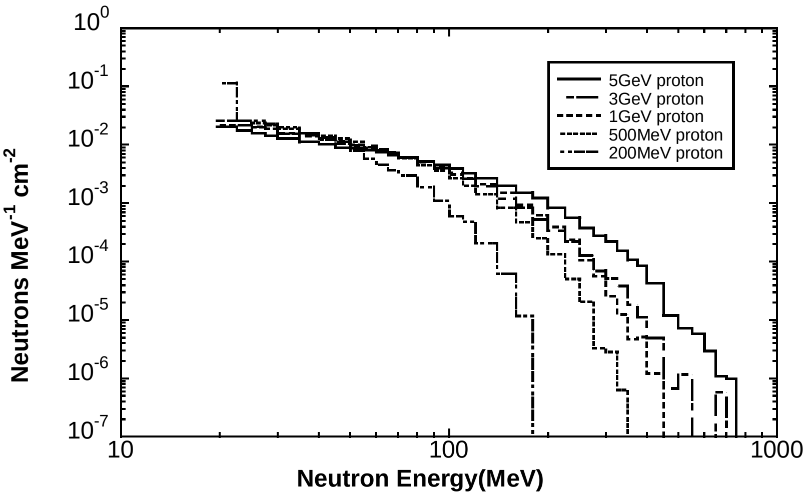

Figure 2. Secondary neutron spectrum from an Hg target bombarded by 3 GeV protons (by MCNPX) and 24 GeV protons (by NMTC/JAM)

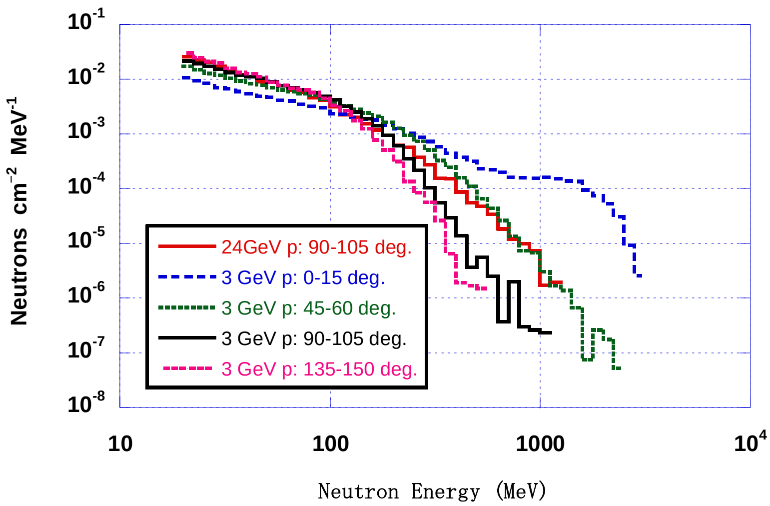

Geometry

The geometry used was plane (6 m thick) with normal incident parallel beams.

Shielding material

As typical shielding materials, iron and concrete were selected. The densities of the two materials were 7.87 g cm P^{-3P} (iron) and 2.27 g cm P^{-3P} (concrete) [Type 02-a, ANL-5800 and 660 (1963)]. The composition of concrete is given in Table 1.

Energy group and fluence-to-dose equivalent conversion factor

The energy group in Table 2 is presented as the standard. If possible, the neutron spectra should be presented in this energy group.

In dose calculations, use of the neutron flux-to-dose equivalent conversion factor (Table 3) is recommended, thus avoiding any ambiguity due to the conversion factor. The values given in Table 3 are conversion factors for the neutron energy corresponding to that given in Table 2.

Table 1. Composition of concrete

Element	Atomic number density (10P^{24P}/cmP^{3P})	Weight per cent	Element	Atomic number density (10P^{24P}/cmP^{3P})	Weight per cent
H	1.3851E-2	1.02	Si	1.6621E-2	34.21
C	1.1542E-4	1.00	K	4.6205E-4	1.32
O	4.5921E-2	53.85	Ca	1.5025E-3	4.41
Mg	1.2388E-4	0.22	Fe	3.4510E-4	1.41
Al	1.7409E-3	3.44	–	–	–

Table 2. Upper energy of 69 neutron energy groups with lower limit of 20 MeV (in MeV)

1.00E+5	9.00E+4	8.00E+4	7.00E+4	6.00E+4	5.00E+4	4.00E+4	3.00E+4	2.00E+4
1.80E+4	1.60E+4	1.40E+4	1.20E+4	1.00E+4	9.00E+3	8.00E+3	7.00E+3	6.00E+3
5.00E+3	4.50E+3	4.00E+3	3.50E+3	3.00E+3	2.50E+3	2.00E+3	1.90E+3	1.80E+3
1.70E+3	1.60E+3	1.50E+3	1.40E+3	1.30E+3	1.20E+3	1.10E+3	1.00E+3	9.00E+2
8.00E+2	7.00E+2	6.00E+2	5.00E+2	4.00E+2	3.75E+2	3.50E+2	3.25E+2	3.00E+2
2.75E+2	2.50E+2	2.25E+2	2.00E+2	1.80E+2	1.60E+2	1.40E+2	1.20E+2	1.10E+2
1.00E+2	9.00E+1	8.00E+1	7.00E+1	6.50E+1	6.00E+1	5.50E+1	5.00E+1	4.50E+1
4.00E+1	3.50E+1	3.00E+1	2.75E+1	2.50E+1	2.25E+1	2.00E+1	–	–

Table 3. Neutron flux-to-dose conversion factor [(Sv/hr)/(n/sec/cmP^{2P})] [7]

1.98E–5	1.96E–5	1.93E–5	1.93E–5	1.90E–5	1.85E–5	1.78E–5	1.58E–5	1.40E–5
1.35E–5	1.30E–5	1.24E–5	1.17E–5	1.09E–5	1.05E–5	1.00E–5	9.55E–6	9.01E–6
8.42E–6	8.11E–6	7.77E–6	7.41E–6	7.02E–6	6.72E–6	6.32E–6	6.22E–6	6.11E–6
5.98E–6	5.84E–6	5.69E–6	5.52E–6	5.34E–6	5.14E–6	4.94E–6	4.72E–6	4.47E–6
4.18E–6	3.78E–6	3.26E–6	2.72E–6	2.25E–6	2.20E–6	2.15E–6	2.10E–6	2.05E–6
1.99E–6	1.93E–6	1.86E–6	1.82E–6	1.79E–6	1.77E–6	1.74E–6	1.72E–6	1.70E–6
1.68E–6	1.67E-6	1.65E–6	1.64E–6	1.63E–6	1.62E–6	1.61E–6	1.60E–6	1.59E–6
1.58E–6	1.57E–6	1.56E–6	1.55E–6	1.54E–6	1.53E–6	1.52E–6	–	–

Quantities to be calculated

The following quantities must be calculated for the comparison: dose equivalent due to neutrons above 20 MeV at 50, 100, 150, 200, 250, 300, 350, 400, 450 and 500 cm; and neutron spectrum in *n* cm $^{-}$P^{2P}MeV^{-1} per source neutron at 100, 200, 300, 400 and 500 cm.

Summary of contributors

Neutron attenuation calculation

The three groups sent their results to Hideo Hirayama at KEK before the end of April 2004. Table 4 lists the participants as well as the computer codes used and their corresponding databases.

Table 4. Summary of contributors

Name of participant and the organisation	Computer code used	Database corresponding to the computer code
H. Nakashima (JAERI)	PHITS [8]	Library data in PHITS
N. Mokhov (FNAL)	MARS14 [9,10,11]	Library data in MARS14
A.M. Voloschenko (Keldysh Institute of Applied Mathematics)	ROZ-6.5 [12,13,14]	SADCO-2

Results and discussions

Attenuation length

The attenuation length (λ, g cm P^{-2P}) for each case was obtained by a least-squares fitting at the region where the dose decreased exponentially. The obtained neutron attenuation lengths for iron and concrete are shown in Figures 3 and 4, respectively.

In the case of iron, the results for PHITS were calculated for a 300 cm slab, and not a 600 cm slab. (In addition to these calculations, Figure 3 also shows the results presented at previous SATIF meetings.) The attenuation lengths for iron are scattered around each other below 500 MeV, but are relatively close above the 1 GeV level, except for the ROZ-6.5 results. Based on the results of MARS14, the attenuation lengths seem to be almost constant above a few GeV. On the other hand, the results of PHITS and NMTC/JAM increase as the source neutrons increase, even above 10 GeV. The attenuation lengths of these results were obtained for the 150 and 300 cm regions. It is assumed that at this depth the neutron spectrum for a high-energy source does not reach equilibrium. This assumption is confirmed by the attenuation lengths between 150 and 300 cm for MARS14 (Figure 4), which is similar to the results of PHITS and NMTC/JAM.

In the case of concrete, the differences in attenuation lengths for each code are relatively small, and do not depend on the source neutron energy, except for the results of ROZ-6.5 above 200 MeV. The attenuation length increases as the source neutrons increase, even at 100 GeV. This tendency can be explained using the same reason as that mentioned in the iron case for the results of NMTC/JAM and PHITS. The quantities related to the neutron interaction depend on the depth in g cm^{-2}, rather than in cm. If we consider the densities of concrete and iron, 600 cm of concrete corresponds to 173 cm of iron. The neutron spectrum in the 300-500 cm region for concrete is not supposed to reach equilibrium for high-energy neutrons above GeV.

The results for ROZ-6.5 are less than those produced by other codes when above several hundreds of MeV. Despite this fact, the results for ROZ-6.5 are very important in this intercomparison, considering that most of the results are based on Monte Carlo methods. We hope that A.M. Voloschenko, *et al.*, will improve their data and continue to contribute to this intercomparison.

Figure 3. Comparison of the attenuation length of iron

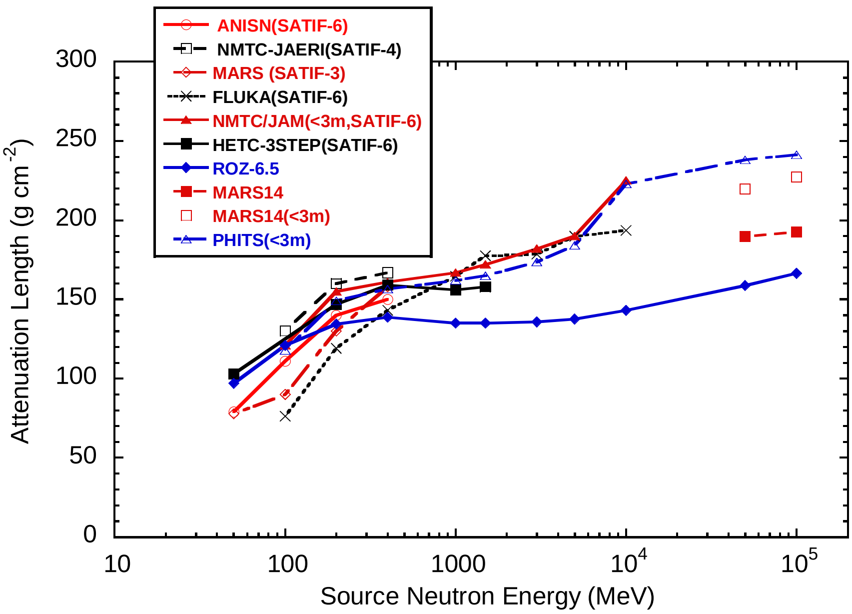

Figure 4. Comparison of the attenuation length of concrete

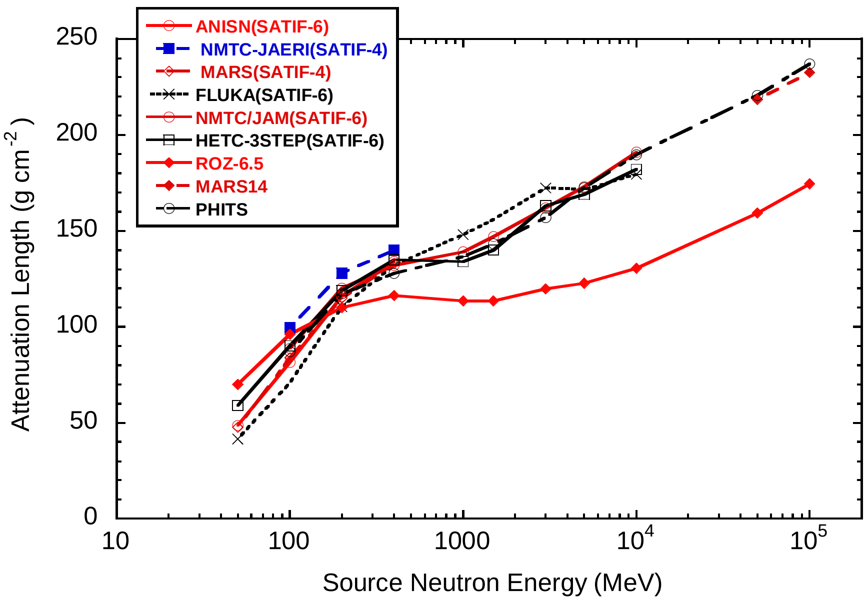

The attenuation lengths of iron and concrete for secondary neutrons from an Hg target with 3 and 24 GeV protons are shown as a function of the emission angle in Figures 5 and 6, respectively. The PHITS results show a similar tendency concerning the values of the attenuation length and their emission angle dependence with those presented at SATIF-6. The results of ROZ-6.5 are smaller than those of other codes, and show a weak dependence on the emission angle. The results for secondary neutrons from 24 GeV protons show a larger attenuation length than those from 3 GeV protons, reflecting the higher energy neutrons shown in Figure 3. The experimental results at ISIS [7] and LANSCE [8] for 800 MeV protons are shown in Figures 5 and 6.

Figure 5. Comparison of the neutron attenuation length of iron for secondary neutrons from an Hg target with 3 and 24 GeV protons

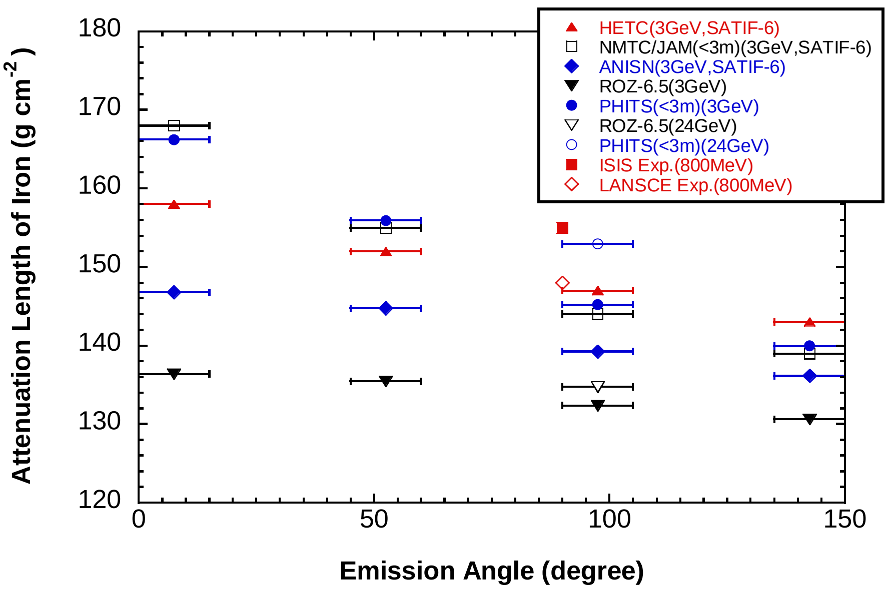

Figure 6. Comparison of the neutron attenuation length of concrete for secondary neutrons from an Hg target with 3 and 24 GeV protons

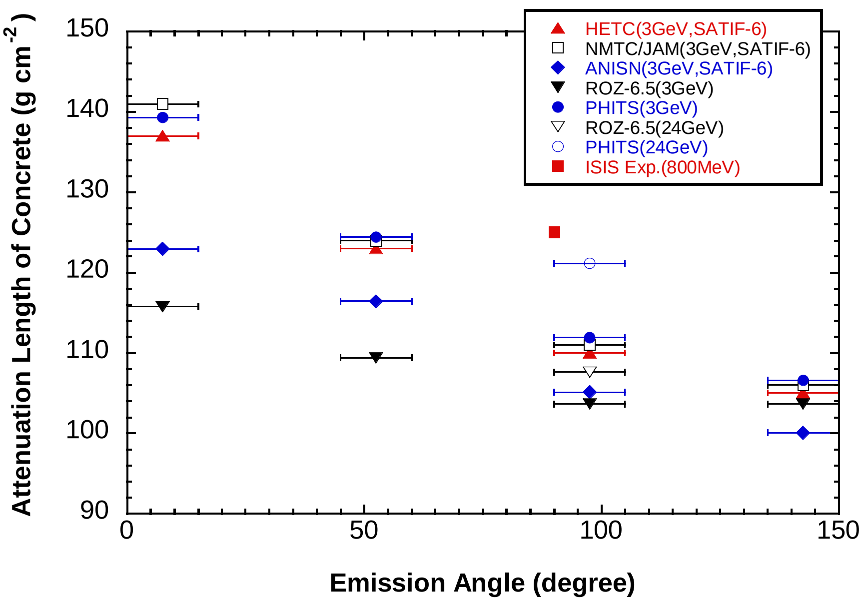

The attenuation lengths of iron and concrete for secondary neutrons from an iron target and from high-energy protons are shown in Figures 7 and 8, respectively. In these figures, the experimental results at ISIS [7] and LANSCE [8] for 800 MeV protons are plotted for comparison. Results of both ROZ-6.5 and PHITS show almost similar values to previous results, except for a slightly weak dependence on the proton energy in the case of ROZ-6.5.

Figure 7. Comparison of the neutron attenuation length of iron for secondary neutrons from an iron target with protons

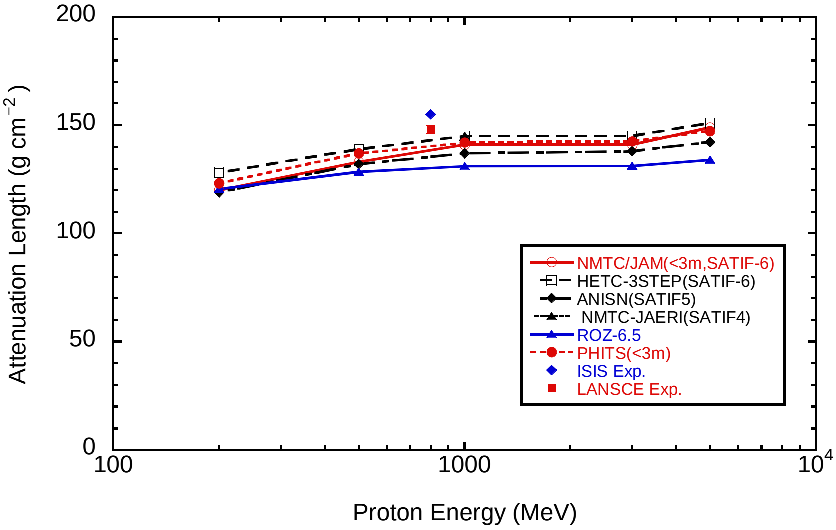

Figure 8. Comparison of the neutron attenuation length of concrete for secondary neutrons from an iron with protons

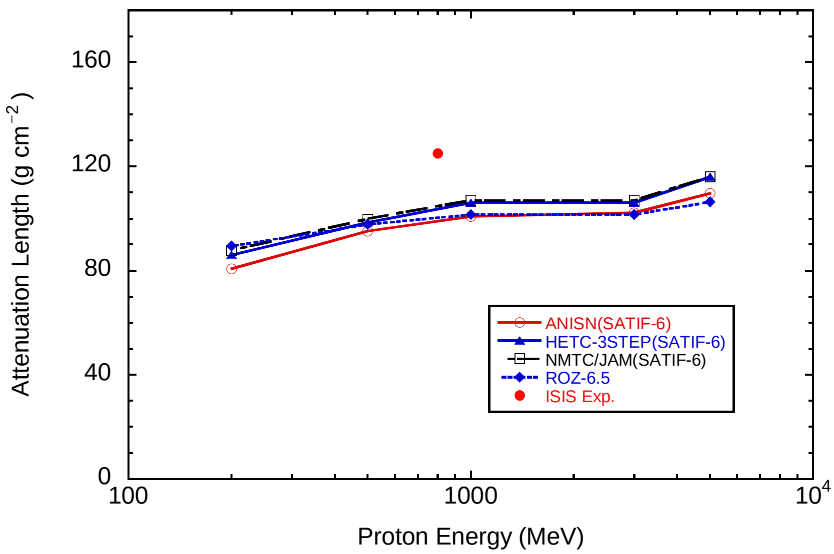

Future themes

From the above comparisons, the following activities should be discussed and performed as the next steps:

A. Compare with the results of other codes to confirm the tendency shown above. It would be desirable to receive results from other groups for comparison.

B. Neutron-dose equivalent attenuation deep inside shields (at 3-5 m for iron and 6-10 m for concrete) in order to confirm that the attenuation length reaches a constant value.

C. Select suitable experiments for comparison in order to understand the attenuation length of secondary neutrons from high-energy protons. The results of AGS shielding experiments presented by H. Nakashima, *et al*., are suitable for this purpose.

D. Dose equivalents are different depending on the code used, which was seen in this intercomparison even for simple problems. Good benchmark experiments are desired to check the models used in each code system.

REFERENCES

[1] Hirayama, H., *et al*., "Inter-comparison of the Medium-energy Neutron Attenuation in Iron and Concrete", *Proceedings of the SATIF-3, Shielding Aspects of Accelerators, Targets and Irradiation Facilities*, Tohoku University, pp. 185-195, 12-13 May 1997.

[2] Hirayama, H., *et al*., "Inter-comparison of the Medium-energy Neutron Attenuation in Iron and Concrete (2)", *Proceedings of the Shielding Aspects of Accelerators, Targets and Irradiation Facilities – SATIF-4*, Knoxville, Tennessee, USA, pp. 143-154, 17-18 September 1998.

[3] Hirayama, H., *et al*., "Inter-comparison of the Medium-energy Neutron Attenuation in Iron and Concrete (3)", *Proceedings of the Shielding Aspects of Accelerators, Targets and Irradiation Facilities – SATIF-5*, Paris, France, pp. 189-201, 18-21 July 2000.

[4] Hirayama, H., *et al*., "Inter-comparison of the Medium-energy Neutron Attenuation in Iron and Concrete (4)", *Proceedings of the Shielding Aspects of Accelerators, Targets and Irradiation Facilities – SATIF-6*, SLAC, USA, 10-12 April 2002.

[5] Maekawa, private communication.

[6] Niita, K., *et al.*, *High Energy Particle Transport Code NMTC/JAM*, JAERI-Data/Code 2001-007 (2001).

[7] ICRP Publication 51, "Data for Use in Protection against External Radiation", *Annals of the ICRP*, 17 (2/3) 1987.

[8] Iwase, H., K. Niita, T. Nakamura, "Development of General-purpose Particle and Heavy Ion Transport Monte Carlo Code", *J. Nucl. Sci. Technol.*, 39, 1142-1151 (2002).

[9] Mokhov, N.V., *The MARS Code System User's Guide*, Fermilab-FN-628 (1995).

[10] Krivosheev, O.E., N.V. Mokhov, "MARS Code Status", *Proc. Monte Carlo 2000 Conf.*, Lisbon, p. 943, 23-26 October 2000; Fermilab-Conf-00/181 (2000).

[11] Mokhov, N.V. *Status of MARS Code*, Fermilab-Conf-03/053 (2003).

[12] Voloschenko, M., A.A. Dubinin, *ROZ-6.5 – One-dimensional Discrete-ordinates Neutron, Photon and Charged Particles Transport Code*, User's Guide, Report No. 7-6-98, Keldysh Institute of Applied Mathematics, Moscow (1998) [in Russian].

[13] Averin, V., A.M. Voloschenko, E.P. Kondratenko, A.A. Dubinin, "The ROZ-6.4 One-dimensional Discrete-ordinates Neutrons, Gamma-rays and Charged Particles Transport Code", *Proc. Int. Topical Meeting on Advances in Mathematics, Computations and Reactor Physics*, Pittsburgh, USA, Vol. 5, pp. 30.3 5-1, 28 April-2 May 1991.

[14] Voloschenko, M., S.V. Gukov, "Some New Algorithms for Solving the Coupled Electron-photon Transport Problems by the Discrete-ordinates Method", *Proc. Int. Conf. on the New Frontiers of Nuclear Technology: Reactor Physics, Safety and High-performance Computing – PHYSOR 2002*, Seoul, Korea, 7-10 October 2002.

[15] Nunomiya, T., *et al*., "Measurement of Deep Penetration of Neutrons Produced by 800 MeV Proton Beam through Concrete and Iron at ISIS", *Nucl. Instr. and Meth.*, B179, pp. 89-102 (2001).

[16] Bull, J.S., J.B. Donahue, R.L. Burman, "Measurement of Neutron Attenuation through Thick Shields and Comparison with Calculation", *Proc. of the 4th Workshop on Simulating Accelerator Radiation Environments – SARE4*, Knoxville, Tennessee, pp. 201-208, 14-16 September 1998.

Annex

PROPOSAL BY ANDREI M. VOLOSCHENKO

It is not a simple task to subdivide high-energy neutrons and protons (and maybe pions) transport when performing target/accelerator radiation shield calculations. The coupled hadron cascade problem should be solved.

Additionally, it is difficult to compare the calculation of problems using a high-energy neutron source only with experimental data, as a real target emits more than just neutrons.

Computers today are quite powerful. As a result, perhaps more realistic and thus more complicated intercomparison problems should be developed. I believe that the beam spill and full stop problems described by H. Handa, *et al.*, in "Deep Penetration Calculations of Neutrons up to 1.5 GeV" from the SATIF-5 proceedings are quite acceptable for intercomparison.

I sent you some results of the 2-D model for the liquid metal target shield calculations. Charged components of radiation cannot be neglected in this calculation, and sufficiently high order angular quadrature and PL approximation of scattering cross-sections should be used to achieve acceptable results.